Coexistence of Two Sharp-Mode Couplings and their Unusual Momentum Dependence in the Superconducting State of $Bi_2Sr_2CaCu_2O_{8+\delta}$ Revealed by Laser-Based Angle-Resolved Photoemission

Junfeng He,[1] Wentao Zhang,[1] Jin Mo Bok,[2] Daixiang Mou,[1] Lin Zhao,[1] Yingying Peng,[1] Shaolong He,[1] Guodong Liu,[1] Xiaoli Dong,[1] Jun Zhang,[1] J. S. Wen,[3] Z. J. Xu,[3] G. D. Gu,[3] Xiaoyang Wang,[4] Qinjun Peng,[4] Zhimin Wang,[4] Shenjin Zhang,[4] Feng Yang,[4] Chuangtian Chen,[4] Zuyan Xu,[4] H.-Y. Choi,[2] C. M. Varma,[5] and X. J. Zhou[1,*]

[1]*National Laboratory for Superconductivity, Beijing National Laboratory for Condensed Matter Physics, Institute of Physics, Chinese Academy of Sciences, Beijing 100080, China*

[2]*Department of Physics and Institute for Basic Science Research, SungKyunKwan University, Suwon 440-746, Korea*

[3]*Condensed Matter Physics and Materials Science Department, Brookhaven National Laboratory, Upton, New York 11973, USA*

[4]*Technical Institute of Physics and Chemistry, Chinese Academy of Sciences, Beijing 100080, China*

[5]*Department of Physics and Astronomy, University of California, Riverside, California 92521, USA*

(Received 2 October 2012; revised manuscript received 12 February 2013; published 5 September 2013)

High-resolution laser-based angle-resolved photoemission measurements have been carried out on $Bi_2Sr_2CaCu_2O_{8+\delta}$ (Bi2212) superconductors to investigate momentum dependence of electron coupling with collective excitations (modes). Two coexisting energy scales are clearly revealed over a large momentum space for the first time in the superconducting state of the overdoped Bi2212 superconductor. These two energy scales exhibit distinct momentum dependence: one keeps its energy near 78 meV over a large momentum space while the other changes its energy from ~40 meV near the antinodal region to ~70 meV near the nodal region. These observations provide a new picture on momentum evolution of electron-boson coupling in Bi2212 that electrons are coupled with two sharp modes simultaneously over a large momentum space in the superconducting states. Their unusual momentum dependence poses a challenge to our current understanding of electron-mode-coupling and its role for high-temperature superconductivity in cuprate superconductors.

DOI: 10.1103/PhysRevLett.111.107005 PACS numbers: 74.72.Gh, 71.38.−k, 74.25.Jb, 79.60.−i

The physical properties of materials are dictated by the interaction of electrons with other entities like other electrons, phonons, magnons, impurities, etc. In particular, the superconductivity of materials involves interaction between electrons that may be direct or indirect through an exchange of a collective excitation (boson) that gives rise to electron pairing [1]. Understanding such many-body effects is essential for understanding the anomalous normal-state properties and superconductivity mechanism in high-temperature cuprate superconductors. With a dramatic improvement of instrumental resolutions, angle-resolved photoemission spectroscopy (ARPES) has become a powerful tool to directly probe many-body effects in cuprate superconductors [2–5]. One prominent case is the observation of a dispersion kink along the (0, 0)–(π, π) nodal direction. This nodal kink is found to be at ~70 meV which is ubiquitous in different materials, different dopings, and at temperatures both above and below the superconducting transition [6–11]. On the other hand, near the (π, 0) antinodal region, a clear dispersion kink at ~40 meV has also been identified [12–16]. In addition to the origin of the nodal 70 meV kink and the antinodal 40 meV kink that remain under debate (magnetic, phononic, or others), a long-standing puzzle to be resolved is their relationship. In particular, how does the 70 meV nodal kink evolve into the antinodal 40 meV kink when the momentum gradually moves from the nodal to the antinodal regions? Investigation of the momentum dependence of the electron interaction is critical in understanding the electron pairing in high-temperature superconductors [17–19].

In this Letter, by carrying out high-resolution ARPES measurements on $Bi_2Sr_2CaCu_2O_{8+\delta}$ (Bi2212) (see Supplemental Material for experimental details [20]), we have revealed for the first time that two prominent energy scales coexist in a large area of momentum space in the superconducting state, especially in overdoped samples. The ~78 meV energy scale is observed over the Fermi surface from nodal to antinodal regions with nearly a fixed energy, while the other energy scale evolves from the antinodal region to the nodal region with its energy varying from ~40 to ~70 meV. These observations provide a new picture on electron-boson coupling in Bi2212. It also provides insight on the unusual nature of these two electron-mode couplings and their possible role in high-temperature superconductivity.

Figure 1(a) shows the photoemission data on the Bi2212 overdoped (OD) 82 K sample measured along an off-nodal momentum cut at 17 K. Two coexisting features can be identified for the first time. In the second-derivative image [Fig. 1(b) for OD82K sample and Fig. 1(c) for OD73K sample] which can enhance the visibility of band

structures, there are two discontinuities observed from the spectral weight distribution of the main band, accompanied by two white lines (spectral peaks) on both the left and right sides of the main band. Quantitative dispersion [Fig. 1(e)] is obtained from fitting the momentum distribution curves (MDCs). By subtracting a straight line as an empirical bare band [red dashed line in Fig. 1(e)], we can get the effective real part of electron self-energy $\mathrm{Re}\Sigma$ [Fig. 1(f) for both OD82K and OD73K]. Two peaks emerge in $\mathrm{Re}\Sigma$: one strong peak at ~50 meV and the other weak one near 78 meV. The feature near 150 meV was observed before [3] and will not be discussed here. Signatures of two features can also be discerned from the corresponding MDC width [Fig. 1(g)]. Particularly, the photoemission spectra [energy distribution curves (EDCs) Figs. 1(h) and 1(i)] show a clear multiple "peak-dip-hump" structure with two dips that are revealed for the first time. The peaks are 5%–10% of the background likely to be beyond any of its variation. Hereafter, for convenience, we call the feature at ~50 meV the LW energy feature, while the other one at ~78 meV as the HI energy feature. It is evident that these two energy features exist in both samples although their relative intensity varies; the HI energy feature is more obvious in the OD73K sample.

Detailed momentum dependent ARPES measurements have been carried out on the OD82K sample to investigate how the two energy features evolve from the nodal to antinodal regions. Figures 2(a1)–2(a5) show the measured data along five momentum cuts; their corresponding EDC second-derivative data are shown in Figs. 2(b1)–2(b5). Except for the nodal cut 1 where the two energy features are too close to be distinguished [Fig. 2(b1)], the two coexisting energy features are clear in all the other images [Figs. 2(b2)–2(b5)]. Two-dip features are also clear in EDCs at the Fermi momenta for all the cuts except for the

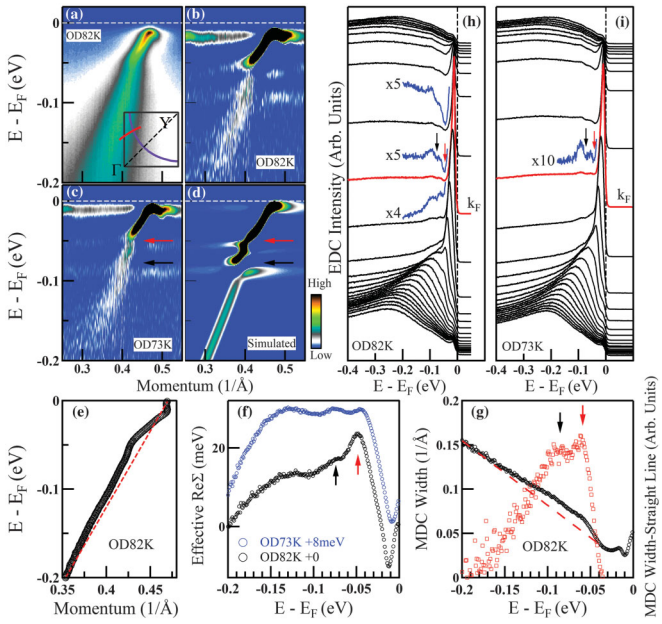

FIG. 1 (color). Identification of two coexisting energy features. (a) Original photoemission data measured at 17 K for OD82K sample. Second-derivative image with respect to energy for OD82K (b) and OD73K (c). (d) Second-derivative image of the simulated single-particle spectral function which considers electron coupling with two Einstein bosonic modes at 50 meV and 78 meV, as indicated by two arrows [20]. (e) Dispersion by MDC fitting for OD82K sample. (f) Effective real part of the electron self-energy for OD82K (black circles) and OD73K (blue circles). (g) MDC width for OD82K (black circle) and the corresponding difference (red square) by subtracting a straight line (red dashed line). (h) and (i) Photoemission spectra (EDCs) showing multiple peak-dip-hump structures for OD82K and OD73K. Typical EDCs at the Fermi momentum (k_F) (red) and near k_F are expended to show the structures more clearly and the arrows indicate the dip positions.

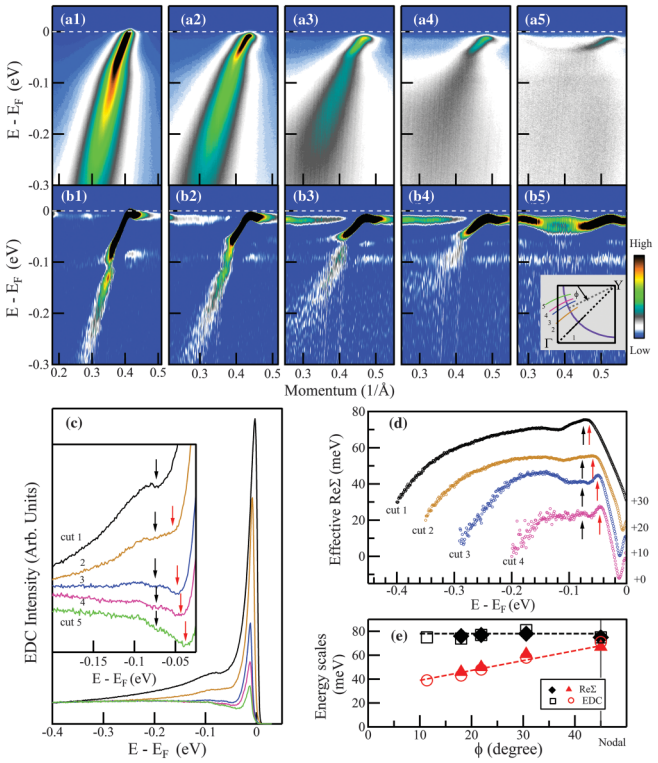

FIG. 2 (color). Momentum dependence of the two energy features in Bi2212 OD82K sample. (a1)–(a5) Original images measured along five momentum cuts at 17 K. (b1)–(b5) Corresponding EDC second-derivative images. The location of the five cuts is shown in the inset. (c) EDCs at the Fermi momenta k_F of these five cuts. Black and red arrows point to the two energy features. (d) Effective real part of electron self-energy of cut 1 to cut 4 [20]. For clarity, they are offset vertically with the offset values shown on the right side. (e) Momentum dependence of the two energy features, extracted from the effective real part of electron self-energy (solid circles and squares) and dip position in EDCs (empty circles and squares). The Φ angle is defined in the inset of (b5) with $\Phi = 45°$ representing the nodal direction.

nodal one because the two energy features become too close [Fig. 2(c)]. The two energy features can also be identified in the effective real part of electron self-energy [Fig. 2(d)]. It is interesting that the LW and HI energy features exhibit different momentum dependence. Figure 2(e) summarizes the position of these two energy features determined from the peak position of the effective real part of electron self-energy (ReΣ) [Fig. 2(d)] and the dip position in the corresponding EDCs [Fig. 2(c)]. The HI energy feature stays near 78 meV and varies little with momentum, while the LW energy feature varies obviously with momentum, dropping from ~67 meV for the nodal cut to ~40 meV (for $\Phi \sim 12°$ cut) near the antinodal region.

Temperature-dependent measurements provide further information on the distinct behaviors of the two energy features, as shown in the effective real part of the electron self-energy measured at different temperatures for three typical momentum cuts (Fig. 3). Both the HI and LW energy features exhibit dramatic superconductivity-induced

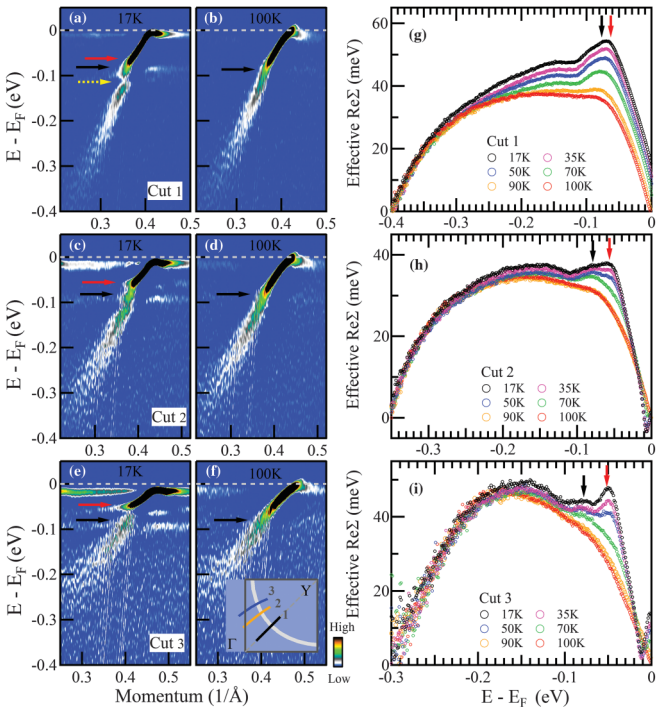

FIG. 3 (color). Temperature dependence of the two types of energy features for the Bi2212 OD82K sample. (a),(b) EDC second-derivative images of cut 1 measured below (at 17 K) and above (at 100 K) T_c. (c),(d) and (e),(f) are the same measurements for cut 2 and cut 3 respectively. (g)–(i) Corresponding effective real part of electron self-energy, measured at different temperatures, for cuts 1, 2, and 3, respectively. For a given cut, a straight line connecting a high binding energy point on the 100 K dispersion and its k_F at the Fermi level is taken as a common empirical bare band for all the temperatures [20]. Peaks of two energy features are marked by arrows, with the red one representing the LW energy feature and the black one representing the HI energy feature.

electron self-energy change upon entering the superconducting state. However, their temperature-dependent behaviors are different. First, the coupling strength of the two energy features exhibit strong momentum dependence, as evidenced by the temperature-induced self-energy change [Figs. 3(g)–3(i)]. For cut 3, near the antinodal region, the superconductivity-induced self-energy change is mainly dominated by the LW energy feature [Fig. 3(i)]. When moving to cut 2, the development of both energy features is clear, but the coupling strength of the LW energy feature appears to get weaker when the momentum moves from the antinodal towards the nodal regions. For cut 1, there is a large superconductivity-induced self-energy change and an apparent existence of the HI energy feature in the normal state. But it is difficult to disentangle whether such a change is caused by HI or LW energy features because they are too close in energy. Second, these two energy features show different temperature dependence across T_c. It is clear from Figs. 3(g) and 3(h) that the HI energy feature is present even in the normal state. The temperature-induced self-energy change takes off even above T_c (82 K), such as the 90 K data in Fig. 3(g), which indicates that the HI energy feature might be caused by a ~70 meV phonon. In contrast, no clear signature of the LW energy feature is observed in the normal state [Fig. 3(i)] and the obvious self-energy enhancement occurs well into the superconducting state (like the data at 50 K and below).

For the doping dependence, Figs. 4(a)–4(c) show the effective real part of electron self-energy along several momentum cuts of Bi2212 overdoped (OD) 82 K, optimally-doped (Opt) 91 K, and underdoped (UD) 89 K samples, and the EDCs at k_F along a typical cut ($\Phi = 18°$) are shown in Fig. 4(d). The LW energy feature and its momentum dependence in the Opt91K [Fig. 4(b)] and UD89K [Fig. 4(c)] Bi2212 samples are similar to that in the OD82K sample [Fig. 4(a)]; it drops in its energy when moving from the nodal region to the antinodal region [Fig. 4(e)]. The signature of the HI energy feature appears rather weak in the Opt91K and UD89K samples, but hint of its existence is discernable. One can also observe double-dip signature in the EDCs of the Opt91K and UD89K samples [Fig. 4(d)] which indicates that the HI feature may extend into the underdoped region. We note that the relative intensity of the HI feature is doping dependent which is enhanced in the overdoped region.

Now, we come to the origin of these two coexisting energy features in the superconducting state, specifically on whether they can be understood by electron coupling with one sharp mode or two. It was shown that the electron coupling with one sharp boson mode (with an energy Ω_0) plus a van Hove singularity near the antinodal $(\pi, 0)$ region at an energy position of $E(\pi, 0)$, can generate two discontinuities in the electron self-energy at $\Omega_0 + E(\pi, 0)$ and $\Omega_0 + \Delta_0$ (with Δ_0 being a superconducting gap) [21]. The resultant two energy scales are expected to be

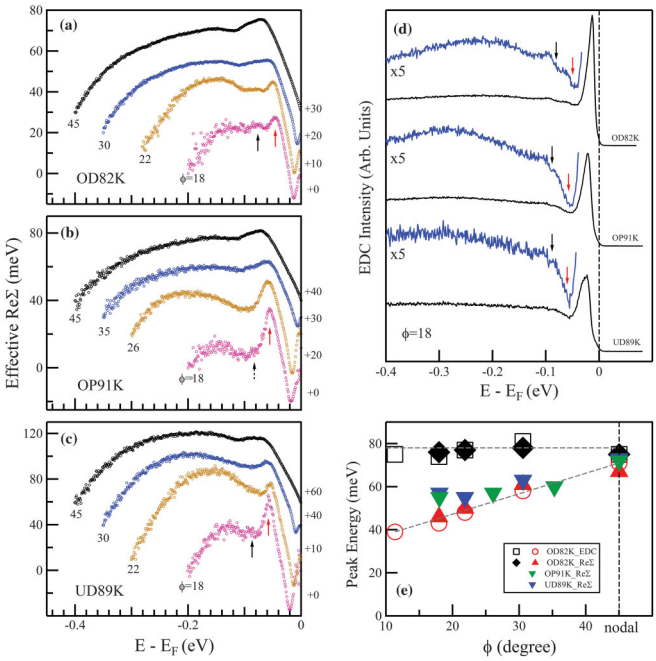

FIG. 4 (color). Doping dependence of the two types of energy features in Bi2212 samples. Effective real part of electron self-energy measured in superconducting state for OD82K sample (a), Opt91K sample (b), and UD89 sample (c) [20]. The location of the momentum cuts are given by Φ angles as defined in Fig. 2(b5). For clarity, the effective real part of electron self-energy is offset vertically with the offset values marked on the right side of the curves. (d) EDCs at the Fermi momentum k_F along the cut $\Phi = 18°$ for the three samples with different doping levels. Part of the EDCs are expanded (blue curves) in order to highlight the possible multiple peak-dip-hump structures. Arrows mark the position of dips. (e) Summary of the momentum dependence of the two types of energy features in Bi2212 with different doping levels. Both EDC and electron self-energy are used to obtain the energy positions.

momentum-independent, and their energy difference, $E(\pi, 0) - \Delta_0$, is expected to be a constant. Our observations of different momentum dependence of the two energy features [Fig. 4(e)] make this one-mode scenario unlikely. They point to electron coupling with two prominent sharp modes. This can be better illustrated by a simulation of the single particle spectral function for the electron coupling with two sharp bosonic modes [Fig. 1(c)] [20]. Even with such a simple model simulation, the similarity of the measured [Fig. 1(b)] and simulated [Fig. 1(c)] images is obvious, and the simulated image serves as a guide for us to extract energy scales from the peak position of the real part of electron self-energy and dip position in EDCs.

Our present work makes it clear that there are two separate energy scales that coexist over a large momentum space, and the evolution of the nodal 70 meV kink to the antinodal 40 meV kink is not a single mode evolution as previously thought. The HI energy scale does not change much in its energy with momentum while the LW energy scale changes its energy from ~70 meV near the nodal region to ~40 meV near the antinodal region. In the nodal region, the usually referred 70 meV kink is actually composed of two coexisting energy scales that are close in energy. Near the antinodal region, the 40 meV kink is obvious because the coupling strength of the LW mode dominates.

The present observations pose a new challenge to our current understanding of mode coupling in the superconducting state of cuprate superconductors. In a conventional picture where the electron-boson coupling vertex $g(\mathbf{k}, \mathbf{q})$ is nearly momentum independent, if there is a mode (with an energy Ω) coupling in the normal state, its energy is expected to be shifted to $\Omega + \Delta_0$ in the superconducting state [21]. This isotropic coupling picture will generate an energy shift Δ_0 over the entire Fermi surface, including the nodal region where the local superconducting gap is zero in a d-wave superconductor like cuprates [21]. Such a picture is apparently not consistent with our observations. As shown in Figs. 3(g)–3(i), the HI energy feature already exists above T_c at ~78 meV; upon cooling into the superconducting state, it stays nearly at the same energy and no signature of a new energy scale appears at 103 meV (with an energy gap of $\Delta_0 \sim 25$ meV for the OD82K Bi2212). While one may still attempt to explain the phenomenon in a conventional picture [22], it was proposed alternatively that this nonenergy shift puzzle of the nodal 70 meV kink can be attributed to a strong momentum-dependent coupling vertex $g(\mathbf{k}, \mathbf{q})$, with a peculiar electron-boson coupling that involves mainly small q forward scattering [23] in which electron scattering occurs in a small local momentum space, and a mode Ω in the normal state would be expected to be shifted by a local energy gap $\Delta(k)$ upon entering the superconducting state [24]. While the forward scattering picture [23,24] seems to solve the nonshift puzzle of the nodal energy scale across T_c because the local gap near the nodal region is zero, it predicts that the mode energy shift will increase from the nodal to the antinodal regions due to the local gap increase in a d-wave superconductor which is not consistent with our current observation that the HI energy scale changes little in energy over a large momentum space. The momentum dependence of the LW energy scale is even more anomalous because, in this case, the energy scale change from 40 meV near the antinodal region to 70 meV near the nodal region is not only different from a constant that is expected from the conventional coupling picture, but is just opposite to what is expected from the forward scattering picture. These observations indicate that the electron-mode coupling in the superconducting state of Bi2212 is rather unusual and asks for further theoretical efforts.

In summary, by taking high-resolution ARPES measurements, we have identified two coexisting sharp mode couplings over a large momentum space in the superconducting state of Bi2212 for the first time. The unusual momentum dependence of these two mode couplings can

not be understood by known theories and poses new challenges to current understanding of electron-boson coupling in the superconducting state. Although our present work does not imply that the two modes are solely responsible for electron paring in the cuprate superconductors, it solves a long-standing puzzle about the momentum evolution between nodal kink and antinodal kink. Their strong coupling in the superconducting state and their unusual momentum and temperature dependence make it clear that such mode coupling should be considered in the electron pairing mechanism, be it pairing mediator or pairing breaker.

We thank Prof. Qianghua Wang for discussions. X. J. Z. acknowledges funding support from NSFC (Grant No. 11190022) and the MOST of China (Programs No. 2011CB921703 and No. 2011CB605903). The work at BNL is supported by the DOE under Contract No. DE-AC02-98CH10886.

*Corresponding author.
XJZhou@aphy.iphy.ac.cn

[1] P. W. Anderson, Science **316**, 1705 (2007).
[2] A. Damascelli , Z. Hussain, and Z.-X. Shen, Rev. Mod. Phys. **75**, 473 (2003); J. C. Campuzano *et al.*, in *The Physics of Superconductors*, edited by K. H. Bennemann and J. B. Ketterson (Springer, New York, 2004), Vol. 2; X. J. Zhou *et al.*, in *Handbook of High-Temperature Superconductivity: Theory and Experiment*, edited by J. R. Schrieffer (Springer, New York, 2007).
[3] W. T. Zhang *et al.*, Phys. Rev. Lett. **100**, 107002 (2008).
[4] I. M. Vishik *et al.*, Phys. Rev. Lett. **104**, 207002 (2010).
[5] N. C. Plumb, T. J. Reber, J. D. Koralek, Z. Sun, J. F. Douglas, Y. Aiura, K. Oka, H. Eisaki, and D. S. Dessau, Phys. Rev. Lett. **105**, 046402 (2010).
[6] P. V. Bogdanov *et al.*, Phys. Rev. Lett. **85**, 2581 (2000).
[7] P. Johnson *et al.*, Phys. Rev. Lett. **87**, 177007 (2001).
[8] A. Kaminski, M. Randeria, J. C. Campuzano, M. R. Norman, H. Fretwell, J. Mesot, T. Sato, T. Takahashi, and K. Kadowaki, Phys. Rev. Lett. **86**, 1070 (2001).
[9] A. Lanzara *et al.*, Nature (London) **412**, 510 (2001).
[10] X. J. Zhou *et al.*, Nature (London) **423**, 398 (2003).
[11] A. A. Kordyuk *et al.*, Phys. Rev. Lett. **97**, 017002 (2006).
[12] A. D. Gromko, A. Fedorov, Y.-D. Chuang, J. D. Koralek, Y. Aiura, Y. Yamaguchi, K. Oka, Y. Ando, and D. S. Dessau, Phys. Rev. B **68**, 174520 (2003).
[13] T. K. Kim, A. A. Kordyuk, S. V. Borisenko, A. Koitzsch, M. Knupfer, H. Berger, and J. Fink, Phys. Rev. Lett. **91**, 167002 (2003).
[14] T. Sato *et al.*, Phys. Rev. Lett. **91**, 157003 (2003).
[15] T. Cuk *et al.*, Phys. Rev. Lett. **93**, 117003 (2004).
[16] T. P. Devereaux, T. Cuk, Z.-X. Shen, and N. Nagaosa, Phys. Rev. Lett. **93**, 117004 (2004).
[17] H. Kamimura, S. Matsuno, Y. Suwa, and H. Ushio, Phys. Rev. Lett. **77**, 723 (1996).
[18] H. C. Krahl, J. A. Müller, and C. Wetterich, Phys. Rev. B **79**, 094526 (2009).
[19] H. Y. Choi, C. M. Varma, and X. J. Zhou, Front. Phys. **6**, 440 (2011).
[20] See Supplemental Material http://link.aps.org/supplemental/10.1103/PhysRevLett.111.107005 for additional information.
[21] A. W. Sandvik, D. J. Scalapino, and N. E. Bickers, Phys. Rev. B **69**, 094523 (2004).
[22] W. S. Lee, W. Meevasana, S. Johnston, D. H. Lu, I. M. Vishik, R. G. Moore, H. Eisaki, N. Kaneko, T. P. Devereaux, and Z.-X. Shen, Phys. Rev. B **77**, 140504(R) (2008).
[23] M. L. Kulic and O. V. Dolgov, Phys. Rev. B **71**, 092505 (2005).
[24] S. Johnston, I. M. Vishik, W. S. Lee, F. Schmitt, S. Uchida, K. Fujita, S. Ishida, N. Nagaosa, Z. X. Shen, and T. P. Devereaux, Phys. Rev. Lett. **108**, 166404 (2012).